Elsevier Editorial System(tm) for Talanta
Manuscript Draft

Manuscript Number: TAL-D-13-02239R1

Title: A novel method for evaluating flavanols in grape seeds by near infrared hyperspectral imaging

Article Type: Research Paper

Keywords: Chemometrics; Flavanols; Grape seeds; Hyperspectral imaging; Near infrared; Vitis vinifera L.

Corresponding Author: Prof. Francisco J. Heredia, PhD

Corresponding Author's Institution: Universidad de Sevilla

First Author: Francisco J. Rodríguez-Pulido, PhD

Order of Authors: Francisco J. Rodríguez-Pulido, PhD; José Miguel Hernández-Hierro, PhD; Julio Nogales-Bueno; Belén Gordillo, PhD; M. Lourdes González-Miret, PhD; Francisco J. Heredia, PhD

Abstract: Chemical composition of seeds changes during grape ripening and this affects the sensory properties of wine. In order to control the features of wines, the condition of seeds is becoming an important factor for deciding the moment of harvesting by winemakers. Sensory analysis is not easy to carry out and chemical analysis needs lengthy procedures, reagents, and it is destructive and time-consuming. In the present work, near infrared hiperespectral imaging has been used to determine flavanols in seeds of red (cv. Tempranillo) and white (cv. Zalema) grapes (Vitis vinifera L.). As reference measurements, the flavanol content was estimated using the p-dimethylaminocinnamaldehyde (DMACA) method. Not only total flavanol content was evaluated but also the quantity of flavanols that would be extracted into the wine during winemaking. A like-wine model solution was used for this purpose. Calibrations were performed by partial least squares regression and they provide coefficients of determination R2=0.73 for total flavanol content and R2=0.85 for predicting flavanols extracted with model solution. Values up to R2=0.88 were reached when cultivars were considered individually.

HIGHLIGHTS

− NIR Hyperspectral imaging was applied to predict the flavanol content in grape seeds.

− The method allows the evaluation of flavanols in grape seeds without sample preparation.

− PLSR predicted total flavanols and flavanols that may be extracted during winemaking.

− The methodology established could be useful for determining the grape harvest.

*Graphical Abstract (for review)

Click here to download high resolution image

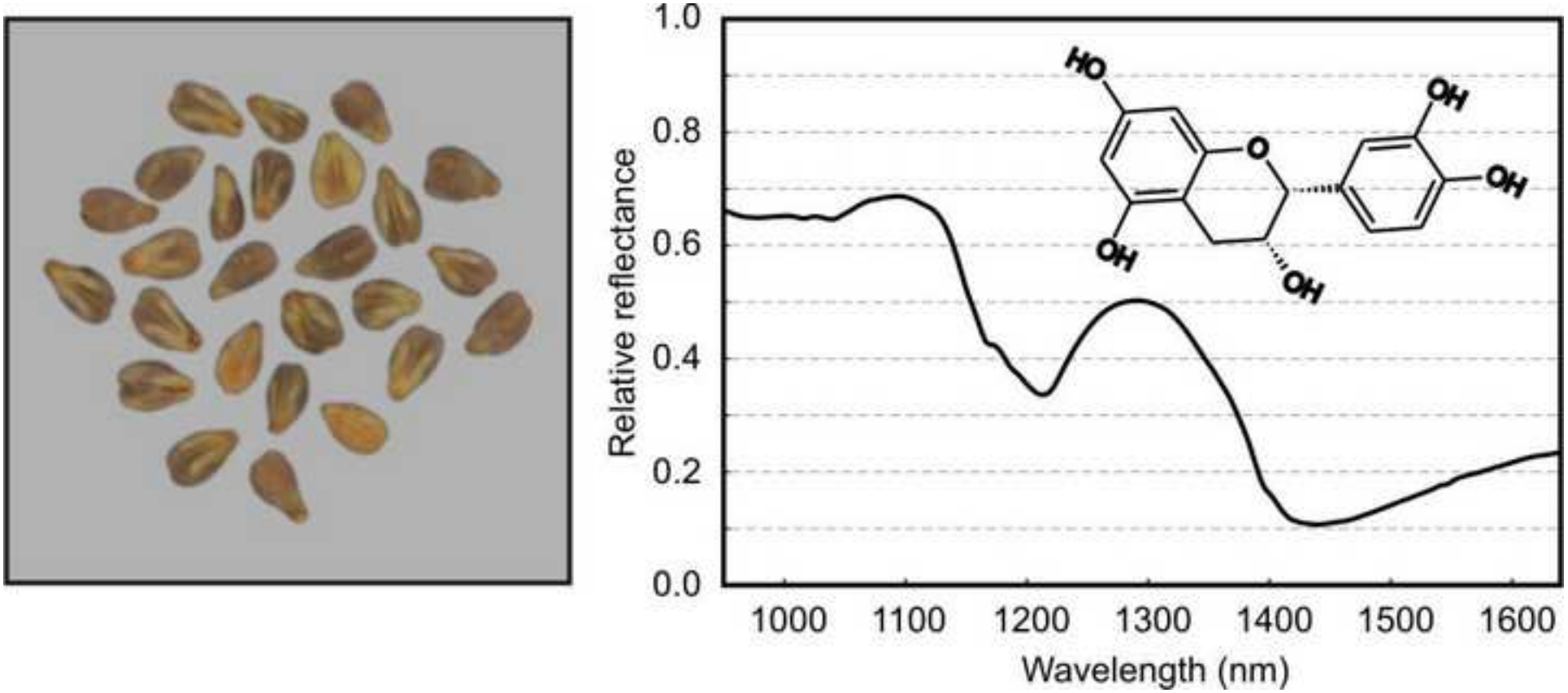

A novel method for evaluating flavanols in grape seeds by near infrared hyperspectral imaging

Rodríguez-Pulido, Francisco J.; Hernández-Hierro, José Miguel; Nogales-Bueno, Julio; Gordillo, Belén; González-Miret, M. Lourdes.; Heredia, Francisco J.

Food Colour & Quality Lab., Dept. Nutrition & Food Science. Facultad de Farmacia. Universidad de Sevilla. 41012-Sevilla, Spain.

Corresponding author:

Heredia, Francisco J.;

Food Colour & Quality Lab., Dept. Nutrition & Food Science. Facultad de Farmacia. Universidad de Sevilla. 41012-Sevilla, Spain

Tel.: +34 954556495 Fax: +34 954556110

e-mail: heredia@us.es

ABSTRACT

Chemical composition of seeds changes during grape ripening and this affects the sensory properties of wine. In order to control the features of wines, the condition of seeds is becoming an important factor for deciding the moment of harvesting by winemakers. Sensory analysis is not easy to carry out and chemical analysis needs lengthy procedures, reagents, and it is destructive and time-consuming. In the present work, near infrared hiperespectral imaging has been used to determine flavanols in seeds of red (cv. Tempranillo) and white (cv. Zalema) grapes (*Vitis vinifera* L.). As reference measurements, the flavanol content was estimated using the *p*-dimethylaminocinnamaldehyde (DMACA) method. Not only total flavanol content was evaluated but also the quantity of flavanols that would be extracted into the wine during winemaking. A like-wine model solution was used for this purpose. Calibrations were performed by partial least squares regression and they provide coefficients of determination R^2=0.73 for total flavanol content and R^2=0.85 for predicting flavanols extracted with model solution. Values up to R^2=0.88 were reached when cultivars were considered individually.

KEYWORDS

Chemometrics; Flavanols; Grape seeds; Hyperspectral imaging; Near infrared; *Vitis vinifera* L.;

1. Introduction

Grape seeds constitute a small part of the berry, but they affect extensively the sensory properties of wine. Their phenolic compounds are responsible of these properties and they change in a qualitative and quantitative manner during ripening [1,2]. The most representative of them in grape seeds, flavanols, include flavan-3-ol monomers (catechin, epicatechin and epicatechin gallate) and procyanidins, which are polymers comprised of flavan-3-ol terminal and extension subunits [3]. Phenolic composition of grapes depends on multiple factors, including climate, variety, soil, and degree of ripeness, being this phenolic maturity decisive for the production of quality red wines. Although seeds represent only 0-6% of berry weight, they are an important source of flavanols for wines. Another aspect that has raised interest is the extractability of these compounds. It has been reported that extractability depends on the ripeness of grape seeds. This phenomenon is due to changes in the interactions between tannins and cell wall material [4]. Insufficiently ripened grapes have higher tannin extractability [5].

The determination of flavanols might help on the decision of the harvest date. However, the 'optimal' harvest date should be defined based on several measurements. Since changes during ripening affect both gustatory and appearance properties, sensorial analysis is the most common approach to evaluate the condition of the seeds by vine growers, though it is difficult to be carried out in an accurate and objective manner [6]. Some studies have found clear evidences relating chemical composition and sensorial parameters in vine products. In particular, flavanols are responsible of these properties in grape

seeds [7-8]. Nevertheless, these methods frequently are destructive, time-consuming, and entail the use of reagents [9-12]. Replacing conventional analyses, near infrared (NIR) spectroscopy provides fast, accurate and non-destructive way to obtain chemical composition [13,14]. These techniques have been successfully joined to computer vision systems [15,16]. NIR radiation has very little energy and penetrates a millimetre or so into the substance depending on the substance's surface composition and structure. Anyhow, phenolic compounds are mainly concentrated within the outer layer of grape seeds [17].

Near-infrared (NIR) hyperspectral imaging is a powerful technique which has been used in several applications in agricultural products [18-22]. In fact, it has been applied to grape seeds for establishing the methodology for acquiring images, discriminating varieties and estimating the date of sampling, but not yet for predicting chemical composition [23]. Hyperspectral imaging provides a digital image and the spectrum belonging to each pixel. Hyperspectral images (HSI), or hypercubes, are three-dimensional data matrix where the first two axes of the matrix represent the spatial coordinates, while the third axis portrays the spectral dimension. They usually are represented as a battery of images where each layer shows the reflectance at a wavelength in grey scale [24]. Due to the great amount of information that they include, HSI require the application of multivariate data analysis for data exploration. As with NIR spectroscopy, chemometric techniques are applied to decompose the image dataset, process and perform regression or classification analyses. The possibilities of hyperspectral imaging based on the NIR range have been illustrated developing

a model able to predict and classify barley kernels [25,26], predicting hardness in maize kernels [27], and studying enzymes activity and detecting sprout damage in wheat [28,29].

In order to minimise contributions from imaging instrument responses that are not related to variations in the composition of the imaged sample, preprocessing of spectral data is often of vital importance if reasonable results are to be obtained from the spectral analysis step. The most frequently used methods for spectral correction are multiplicative scatter correction (MSC), standard normal variate (SNV) and derivation. [30-33]. However, there is still no standard procedure to decide which spectral processing produce best results. Partial least squares regression (PLSR) is a procedure used to relate a large number of independent variables (predictors) to one (PLSR1) or few (PLRS2) response variables (observations) when a reduced number of cases are available. Since it reduces a great number of redundant information, it is very effective in spectral analysis [34,35].

The aim of this work was to evaluate the potential of NIR hyperspectral imaging for the evaluation of flavanols in seeds from red and white grapes during ripening. Hyperspectral imaging was chosen as the best option for evaluating reflectance spectrum in grape seeds because of their heterogeneity and reduced size. Measurements by bulk NIR spectroradiometry need an amount of sample that covers the whole spot of measurement. In this case, the seeds contain interstitial spaces that produce shadows affecting the spectrum intensity. Imaging techniques allow measuring a maximum area of sample without the influence of shadows.

2. Material and methods

2.1 Sampling

The grapes (*Vitis vinifera* L.) sampled are included under the "Condado de Huelva" Designation of Origin, in Southwestern Spain, harvested in 2012. One red variety (cv. Tempranillo) and one autochthonous white variety (cv. Zalema) were used. The number of samples was 18 for Zalema and 15 for Tempranillo, depending on the availability and harvesting times of each variety. They were taken twice a week from early July until postharvest mid-September. Sampling process was carried out at daybreak by taking a pair of berries from alternate grapevines, from four rows of vines, and from both sides of each row up to reach 2 kg of berries. In this process, the berries were taken with pedicel intact to slow down the berry oxidation as long as possible. Once in laboratory, one hundred berries were randomly taken and seeds removed, left to dry at room temperature for 2 hours, and frozen at −20ºC until acquisition of hyperspectral images and chemical analysis. Each sample was divided into three parts used as replicates ((18+15)×3=99 samples). Two of these replicates were allocated to the calibration set and the other sample to the prediction set.

2.2 Hyperspectral image analysis

The system comprised a Xenics® XEVA-USB InGaAs camera (320 × 256 pixels; Xenics Infrared Solutions, Inc., Leuven, Belgium), a spectrograph (Specim ImSpector N17E Enhanced; Spectral Imaging Ltd., Oulu, Finland) covering the spectral range between 884 and 1717 nm (spectral resolution of 3.25 nm), two

70W tungsten iodine halogen lamps (Prilux®, Barcelona, Spain) used as light source, a mirror scanner (Spectral Imaging Ltd., Oulu, Finland), and a computer system. HSI were recorded using a 50 Hz frame rate and an exposure time of 9 ms using the instrument acquisition software SpectralDAQ 3.62 (Spectral Imaging Ltd., Oulu, Finland). From the acquired HSI, it was observed that the first and the last twenty bands of the image had a high level of noise, thus not being useful for spectral data extraction. Therefore, images were cropped to the spectral range of 950-1650 nm with a total of 215 bands.

A 'white reference' image (*W*, 100% reflectance) was acquired from a white Spectralon® ceramic tile (Labsphere Inc., North Sutton, USA), and a 'dark reference' image (*B*, 0% reflectance) was obtained with the light source off and the mirror scanner completely covered with its opaque cap. The white and dark 'reference' HSI were used to correct the raw images (R_0) in order to obtain a relative reflectance image (*R*) according to the following equation:

$$R = \frac{R_0 - B}{W - B} \quad (1)$$

For segmentation of HSI, a method based on forward stepwise discriminant analysis was applied with the software Statistica 8.0 [36]. Image processing, spectral processing and statistical treatment were carried out using MATLAB R2012b [37]. A flowchart of the image processing and spectral treatment used in this study is schematized in Figure 1.

2.3 Chemical analysis

Each sample was split into two fractions subjected to different extractions. For the exhaustive extraction, grape seeds were freeze-dried and ground to obtain a homogeneous powder for extraction. One gram of seed powder was extracted with ten millilitres of methanol:water (75:25), sonicated (15 minutes) and centrifuged (15 minutes), repeating the extraction process twice more. The methanolic extracts were combined and finally made up to 50 mL with methanol. For the extraction in wine-like medium, two grams of intact grape seeds were macerated in 50 mL of model wine solution (4 $g \cdot L^{-1}$ tartaric acid, 12.5% ethanol, adjusted at pH 3.6 with NaOH 0.5 M) during 72 h [38].

Flavanols spectrophotometric analysis of both extractions was carried out following a modification of Vivas et al. [39]. Ten or twenty microlitres of total extraction or wine like medium extracts were mixed with 190 or 180 µL of methanol respetively and 1 mL of DMACA reagent. The DMACA reagent was prepared immediately before use, containing 0.1% (w/v) DMACA (4-dimethylaminocinnamaldehyde) in a mixture of HCl:methanol (1:10, v/v). The analyses were performed in triplicate on an Agilent 8453 UV-visible spectrophotometer (Palo Alto, USA), equipped with diode array detection (DAD), measuring absorbance at 640 nm and using a calibration curve of (+)-catechin (Sigma-Aldrich, St. Louis, USA) for quantification. The aforesaid extract volumes were appropiately modified when the concentration was outside the linear range of the calibration curve. All results were expressed as mg of catechin equivalents per gram of grape seed.

3. Results and discussion

3.1 Segmentation by discriminant analysis

A set of reflectance spectra belonging to seeds and background was collected as input data set. The forward stepwise discriminant analysis included sequentially three wavelengths, 1216, 1392, and 1147 nm for discriminating the region of interest from the background. Figure 2 shows the average spectra belonging to seeds and background (a homogeneous surface composed of polyethylene) and highlights the selected bands. The algorithm of segmentation saved all the masks of segmentation and they were visually supervised for ensuring the suitability of the proposed method.

3.2 Exploratory Analysis of Spectra

Figure 3 shows the mean and standard deviation spectra regarding the variety of grape seeds. It also shows the spectra after applying the transformations Log(1/R), SNV treatment, and second derivative, treatments that yielded the best results in prediction analyses. It can be seen that seeds from white and red grapes have different reflectance intensities along some wavelength regions, although with the same pattern.

Before the quantitative analysis, principal component analysis (PCA) was used as unsupervised pattern recognition technique in order to get information about the latent structure of the spectral matrix. This method provided not only information related to spectral outliers and the distribution of samples in the newly-created space but also was an important source of knowledge with which to evaluate the suitability of prediction set used in PLSR. For detecting possible

outliers, Hotelling's T^2 statistic was used as a measure of the multivariate distance of each sample from the centre of the data set [40]. Regarding the spectral features of each sample, this test rejected 4 of the 99 samples considering a confidence level of 95%. Using the spectral data of the remaining samples (without outliers), PCA was applied again in order to ensure the representativeness of the prediction set in the generated multivariate space.

PC1, PC2, and PC3 explained 98.61%, 1.18%, and 0.10% of the total variance respectively. PC1 was influenced by the time in an extensively manner. Figure 4a shows PC1 and its evolution over time. At every date, spectra from Tempranillo seeds had higher scores than Zalema ones. Moreover, this dependency seemed stronger for Tempranillo, being its slope higher. Figure 4b shows the scatterplot of scores for PC2 and PC3. Generally, Tempranillo seeds presented positive scores for PC2 while Zalema seeds presented negative ones. Furthermore, it can be observed that samples belonging to prediction set were uniformly distributed among calibration set samples. These results are in agreement with results previously reported [23].

3.3 Quantitative analysis

Flavanols content decreased during the grape ripening regardless the variety and type of extraction. The methanol extract flavanols ranged from 4.28 to 34.26 $mg \cdot g^{-1}$ of grape seed. The flavanols from the extracts obtained using like-wine solution ranged from 0.12 to 7.21 $mg \cdot g^{-1}$ of grape seed. Table 1 shows a brief resume of the aforementioned results. It must be highlighted that high standard deviations were due to the evolution during ripeness instead of errors

of measurements. Although it was not the goal of this work, extractability of each sample was evaluated as the fraction of flavanols extracted by the model solution with respect to the exhaustive extraction. The extractability also decreased during ripening, being about 25% at the first stages and about 5% in the last ones.

Results of chemical analyses were used as dependent (Y) variables and the matrix of processed spectra was used as the independent (X) variables in the PLSR. The statistical parameters of the final calibration equations are shown in Table 2. For extractions with methanol and considering all samples as a unique data set, R^2 was 0.73 for calibration and 0.75 for prediction. The RMSEC and RMSEP were 4.01 and 3.86 $mg \cdot g^{-1}$ of grape seed respectively. Results for predicting flavanols extracted by like-wine solution had R^2=0.82 for calibration and R^2=0.85 for prediction. In this case, RMSEC and RMSEP were 0.92 and 0.88 $mg \cdot g^{-1}$ of grape seed respectively. Since cultivar was a determining factor in the preliminary exploratory analysis, the PLSR were repeated for each variety individually. Because of this, results in Tables 1 and 2 are also broken down into varieties. As it was expected, coefficients of determination increased while RMSEC and RMSEP decreased.

Figure 5 shows the loadings resulting of the PLSR model for total flavanols and it indicates the most dominant wavelengths. The spectral region between 1100-1300 nm showed important contribution to the model loadings and is mainly related to the combination band of O-H symmetric and anti-symetric stretching vibration, the combination band of C-H aromatic second overtone, and C-H third overtone vibration. These can be attributed to the chemical structure of phenolic

compounds [41,42]. The first O-H stretching overtone contributes to spectrum at 1400 nm, hence the moisture affects expansively to this band. In this case, the influence can be attributed to the loss of water that grape seeds suffer at the same time that flavanols develop [43]. According to Goodchild *et al.* [44], bands close to 1600 nm are attributed to condensed tannins.

4. Conclusions

The PLSR models were successfully performed to evaluate flavanols in grape seeds. These were able to predict the concentration of flavanols of a sample based on spectral features as the predictor variables with a coefficient of determination of R^2 of 0.75 for total extractions and 0.85 for extractions with model wine solution. Furthermore, this coefficient reached up to 0.88 when varieties were considered individually. On the other hand, PCA was suitable for grape seeds characterization regarding the variety, proving the suitability of the methodology previously established.

It is well known that in the case of agricultural products the range of the variability should be as large as that expected in any future samples. In this work, seeds from different cultivars have been collected during ripening; therefore this variability should be enough to develop models in a feasibility study. Nonetheless, a comprehensive study must be made in order to evaluate other factors such as different production areas, vintages and varieties, for the complete development of these models. Though it is not yet a substitute for conventional chemical analysis, it arises as an attractive alternative due to its simplicity and quickness. By establishing the variables that affects each cultivar,

this could become a reference method to assess the chemical characteristics of grape seeds during maturation, being very useful for vine growers and wineries.

Acknowledgements

This work was supported by the projects P10-AGR6331 (Consejería de Economía, Innovación, Ciencia y Empresa, Junta de Andalucía), AGL2011-30254-C02 (Ministerio de Economía y Competitividad, Gobierno de España). The Spanish MICINN is also thanked for F.J. Rodríguez-Pulido, J. Nogales-Bueno FPI grants (BES-2009-025429 and BES-2012-060192 respectively) and J.M. Hernández-Hierro 'Juan de la Cierva' contract (JCI-2011-09201).

References

[1] Y. Cadot, M.T. Miñana-Castelló, and M. Chevalier, Journal of Agricultural and Food Chemistry, 54 (2006) 9206-9215.

[2] B.S. Sun, T. Pinto, M.C. Leandro, J.M. Ricardo-Da-Silva, and M.I. Spranger, Am. J. Enol. Vitic., 50 (1999) 179-184.

[3] R. Ristic and P.G. Iland, Australian Journal of Grape and Wine Research, 11 (2005) 43-58.

[4] R.L. Hanlin, M. Hrmova, J.F. Harbertson, And M.O. Downey, Australian Journal of Grape and Wine Research, 16 (2010) 173-188.

[5] C. Peyrot des Gachons and J.A. Kennedy, Journal of Agricultural and Food Chemistry, 51 (2003) 5877-5881.

[6] J. Rousseau and D. Delteil, Revue française d'oenologie, 183 (2000) 10-13.

[7] R. Gawel, Australian Journal of Grape and Wine Research, 4 (1998) 74-95.

[8] R. Ferrer-Gallego, M. García-Marino, J.M. Hernández-Hierro, J.C. Rivas-Gonzalo and M.T. Escribano-Bailón, Analytica Chimica Acta, 660 (2010) 22-28.

[9] A.K. Sandhu and L. Gu, Journal of Agricultural and Food Chemistry, 58 (2010) 4681-4692.

[10] T. Fuleki and J.M. Ricardo da Silva, Journal of Agricultural and Food Chemistry, 45 (1997) 1156-1160.

[11] J.A. Kennedy, M.A. Matthews, and A.L. Waterhouse, Phytochemistry, 55 (2000) 77-85.

[12] E. Obreque-Slier, A. Peña-Neira, R. López-Solís, F. Zamora-Marín, J.M. Ricardo-da Silva, and O. Laureano, Journal of Agricultural and Food Chemistry, 58 (2010) 3591-3599.

[13] B.M. Nicolaï, K. Beullens, E. Bobelyn, A. Peirs, W. Saeys, K.I. Theron, and J. Lammertyn, Postharvest Biology and Technology, 46 (2007) 99-118.

[14] J.M. Hernández-Hierro, J. Valverde, S. Villacreces, K. Reilly, M. Gaffney, M.L. González-Miret, F.J. Heredia, and G. Downey, Journal of Agricultural and Food Chemistry, 60 (2012) 7352-7358.

[15] D.F. Barbin, G. ElMasry, D.W. Sun, and P. Allen, Food Chemistry, 138 (2013) 1162-1171.

[16] D.W. Sun, Journal of Food Engineering, 61 (2004) 1-2.

[17] J.H. Thorngate and V.L. Singleton, Am. J. Enol. Vitic., 45 (1994) 259-262.

[18] T.M. Baye, T.C. Pearson, and A.M. Settles, Journal of Cereal Science, 43 (2006) 236-243.

[19] M.A. Shahin and S.J. Symons, Computers and Electronics in Agriculture, 75 (2011) 107-112.

[20] S. Cubero, N. Aleixos, E. Moltó, J. Gómez-Sanchis, and J. Blasco, Food Bioprocess Technol, 4 (2011) 487-504.

[21] D. Lorente, N. Aleixos, J. Gómez-Sanchis, S. Cubero, O.L. García-Navarrete, and J. Blasco, Food Bioprocess Technol, 5 (2012) 1121-1142.

[22] A. Baiano, C. Terracone, G. Peri, and R. Romaniello, Computers and Electronics in Agriculture, 87 (2012) 142-151.

[23] F.J. Rodríguez-Pulido, D.F. Barbin, D.W. Sun, B. Gordillo, M.L. González-Miret, and F.J. Heredia, Postharvest Biology and Technology, 76 (2013) 74-82.

[24] J. Burger and P. Geladi, Analyst, 131 (2006) 1152-1160.

[25] L. Munck and B. Møller, Journal of the Institute of Brewing, 110 (2004) 3-17.

[26] P. Engelbrecht, M. Manley, P.J. Williams, G.D. Toit, and P. Geladi, Pre-germination detected in whole cereal grains using near infrared hyperspectral imaging, *Proceedings of the CST SA - ICC International Grains Symposium,* Quality and Safety of Grain Crops and Foods, 2010, pp. 123-127.

[27] P. Williams, P. Geladi, G. Fox, and M. Manley, Analytica Chimica Acta, 653 (2009) 121-130.

[28] J. Xing, S. Symons, M. Shahin, and D. Hatcher, Biosystems Engineering, 106 (2010) 188-194.

[29] J. Xing, P. Van Hung, S. Symons, M. Shahin, and D. Hatcher, Sensing and Instrumentation for Food Quality and Safety, 3 (2009) 211-218.

[30] P. Geladi, D. MacDougall, and H. Martens, Appl. Spectrosc., 39 (1985) 491-500.

[31] T. Isaksson and T. Næs, Appl. Spectrosc., 42 (1988) 1273-1284.

[32] M. Kaihara, T. Takahashi, T. Akazawa, T. Sato, and S. Takahashi, Spectroscopy Letters, 35 (2002) 369-376.

[33] C. Pizarro, I. Esteban-Díez, A.J. Nistal, and J.-M. González-Sáiz, Analytica Chimica Acta, 509 (2004) 217-227.

[34] P. Lin, Y. Chen, and Y. He, Food and Bioprocess Technology, 5 (2012) 235-242.

[35] M.M. Pojic and J.S. Mastilovic, Food and Bioprocess Technology, 6 (2013) 330-352.

[36] StatSoft Inc.. Statistica 8.0. 2007. Tulsa, USA, StatSoft Inc.

[37] The Mathworks. MATLAB R2012b. 2012. Natik, USA, The MathWorks Inc.

[38] A.B. Bautista-Ortín, P. Rodríguez-Rodríguez, R. Gil-Muñoz, E. Juménez-Pascual, N. Busse-Valverde, A. Martínez-Cutillas, J.M. López-Roca, and E. Gómez-Plaza, Australian Journal of Grape and Wine Research, 18 (2012) 123-130.

[39] N. Vivas, Y. Glories, L. Lagune, C. Saucier, and M. Augustin, Journal International des Sciences de la Vigne et du Vin, 28 (1994) 319-336.

[40 J.E. Jackson, A User's Guide to Principal Components, Wiley, 2005.

[41] L. Bokobza, in: H. W. Siesler, Y. Ozaki, S. Kawata, and H. M. Heise (Eds.), Near-Infrared Spectroscopy: Principles, Instruments, Applications, Wiley-VCH Verlag GmbH, Weinheim, Germany, 2007, pp. 11-41.

[42] R. Ferrer-Gallego, J.M. Hernández-Hierro, J.C. Rivas-Gonzalo, and M.T. Escribano-Bailón, LWT - Food Science and Technology, 44 (2011) 847-853.

[43] B.G. Osborne, T. Fearn, and P.T. Hindle, Practical NIR Spectroscopy With Applications in Food and Beverage Analysis, Longman Group, United Kingdom 1993.

[44] A.V. Goodchild, F.J. El Haramein, A. Abd El Moneim, H.P.S. Makkar, and P.C. Williams, Journal of Near Infrared Spectroscopy, 6 (1998) 175-181.

FIGURE CAPTIONS

Figure 1. Flow chart of the image processing and spectral treatment used in this study.

Figure 2. Spectra of seeds and background highlighting the bands included by the forward stepwise discriminant analysis.

Figure 3. Average reflectance spectra and average processed spectra of each variety. Shaded areas represent the standard deviation at each wavelength.

Figure 4. (a) Dependency of PC1 with date. (b) Scatterplot of scores for PC2 and PC3. Circles represent Zalema and squares represent Tempranillo, in turn, filled and unfilled marks belong to calibration and prediction sets respectively.

Figure 5. Loadings plot for the first three PLS Factors of the regression model for total flavanols prediction.

Table 1

Table 1. Summary of chemical analyses for all samples and regarding the variety (all results were expressed as mg of catechin equivalents per gram of grape seed).

	N	Extraction	Mean	Minimum	Maximum	Std.Dev.
All Samples	95	model wine	2.26	0.12	7.21	2.22
		total	15.82	4.28	34.26	7.74
Zalema	50	model wine	2.54	0.38	6.48	2.40
		total	15.85	5.63	28.05	6.93
Tempranillo	45	model wine	1.95	0.12	7.21	1.98
		total	15.78	4.28	34.26	8.63

Table 2

Table 2. Calibration and prediction results for the PLS models obtained from processed spectra (all results were expressed as mg of catechin equivalents per gram of grape seed).

	N	Extraction	PLS Factors	R^2_C	RMSEC	R^2_P	RMSEP
All samples	95	model wine	3	0.82	0.92	0.85	0.88
		total	3	0.73	4.01	0.75	3.86
Zalema	50	model wine	2	0.83	0.98	0.85	0.92
		total	1	0.82	2.90	0.82	2.93
Tempranillo	45	model wine	2	0.88	0.67	0.88	0.69
		total	6	0.94	2.09	0.88	2.89

Figure 1

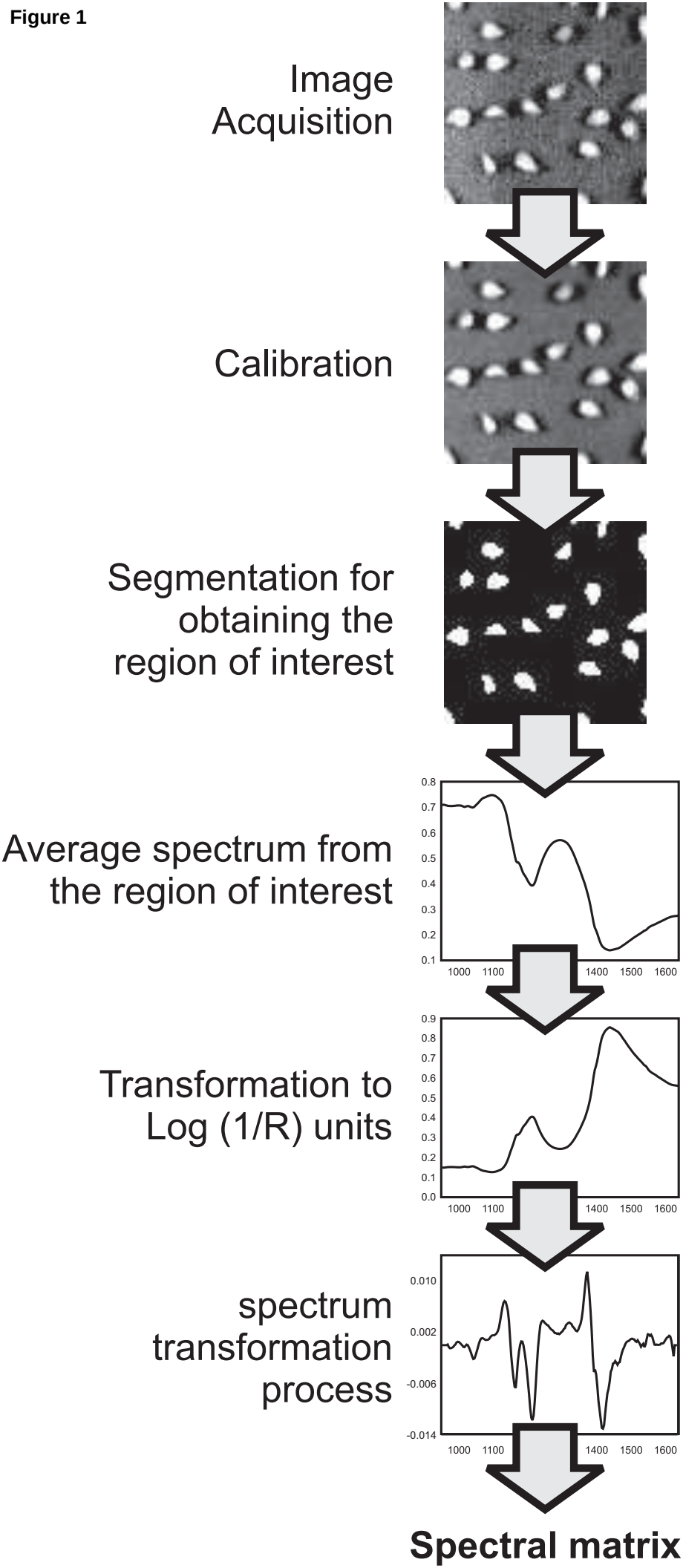
Image Acquisition
Calibration
Segmentation for obtaining the region of interest
Average spectrum from the region of interest
Transformation to Log (1/R) units
spectrum transformation process
0.8
0.7
0.6
0.5
0.4
0.3
0.2
0.1
1000
1100
1400
1500
1600
0.9
0.8
0.7
0.6
0.5
0.4
0.3
0.2
0.1
0.0
0.010
0.002
-0.006
-0.014
Spectral matrix

Figure 2

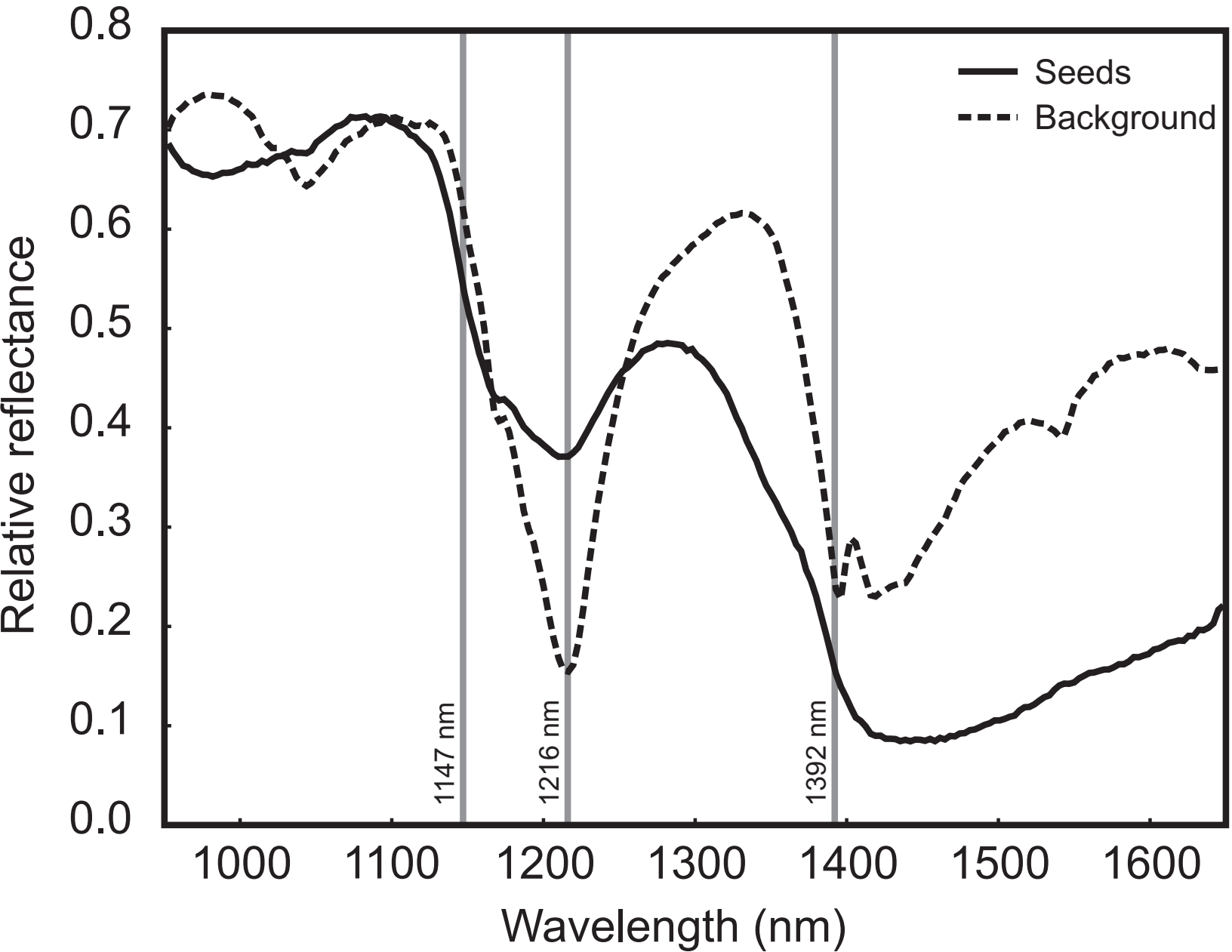
Seeds
Background
Relative reflectance
0.0
0.1
0.2
0.3
0.4
0.5
0.6
0.7
0.8
1147 nm
1216 nm
1392 nm
1000
1100
1200
1300
1400
1500
1600
Wavelength (nm)

Figure 3

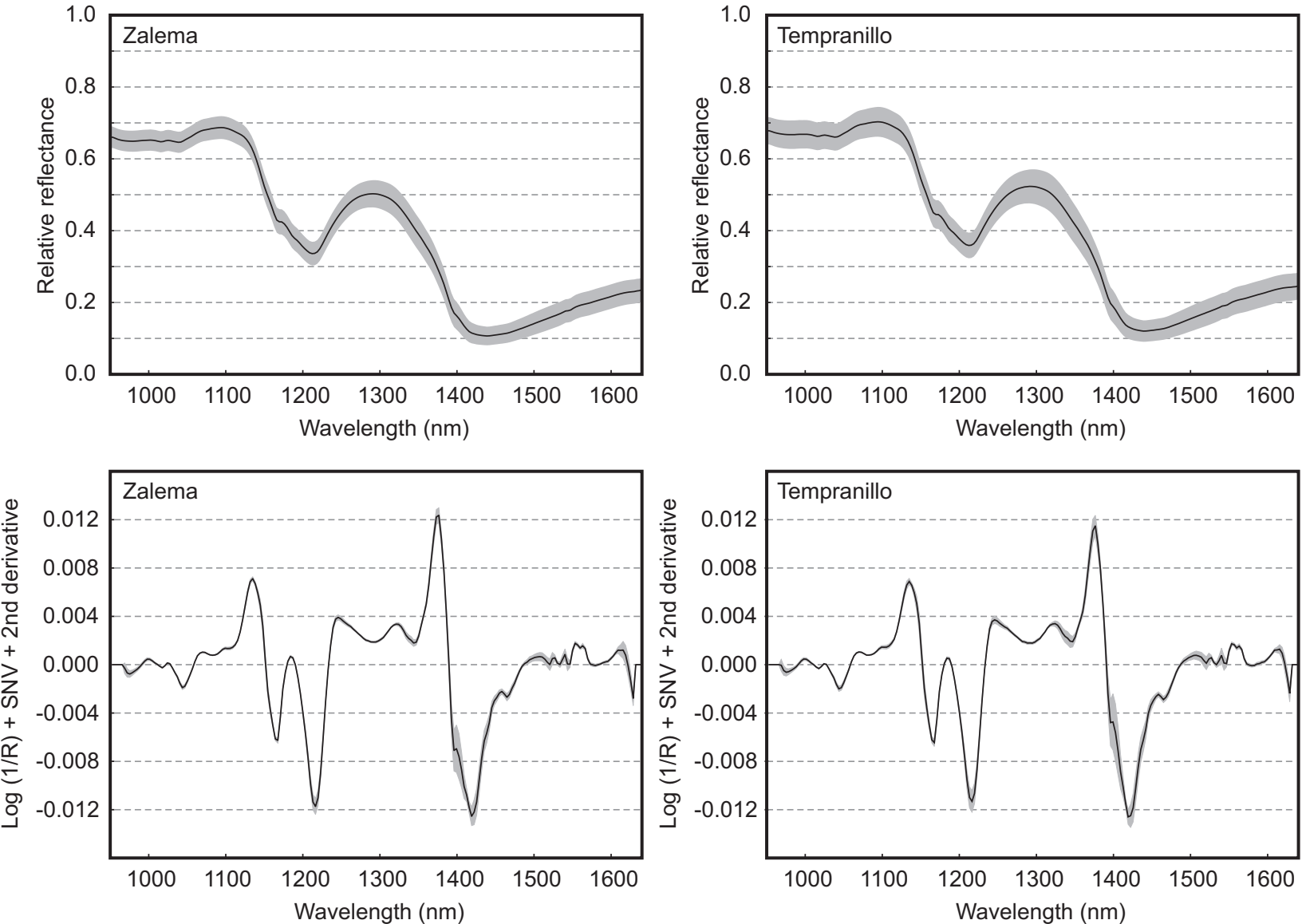
Zalema
Tempranillo
Relative reflectance
Log (1/R) + SNV + 2nd derivative
Wavelength (nm)
1.0
0.8
0.6
0.4
0.2
0.0
0.012
0.008
0.004
0.000
-0.004
-0.008
-0.012
1000
1100
1200
1300
1400
1500
1600

Figure 4

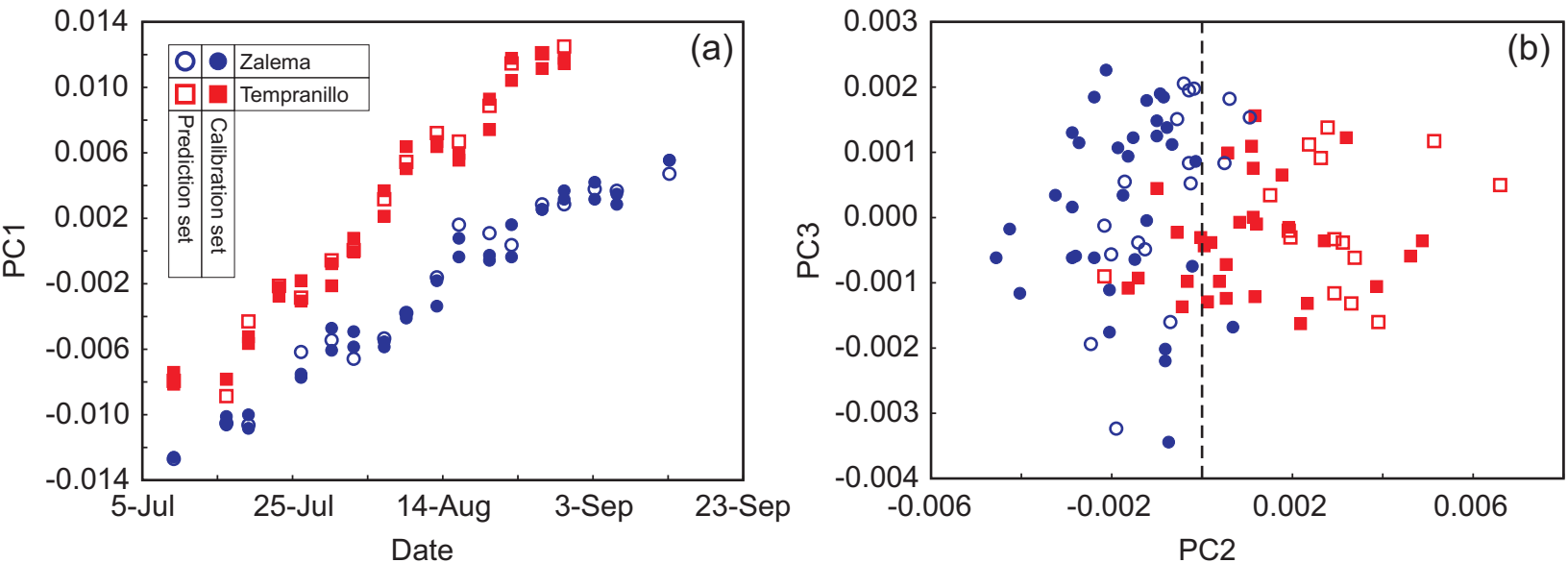
(a)
Zalema
Tempranillo
Calibration set
Prediction set
PC1
0.014
0.010
0.006
0.002
-0.002
-0.006
-0.010
-0.014
5-Jul
25-Jul
14-Aug
3-Sep
23-Sep
Date
(b)
PC3
0.003
0.002
0.001
0.000
-0.001
-0.002
-0.003
-0.004
-0.006
-0.002
0.002
0.006
PC2

Figure 5

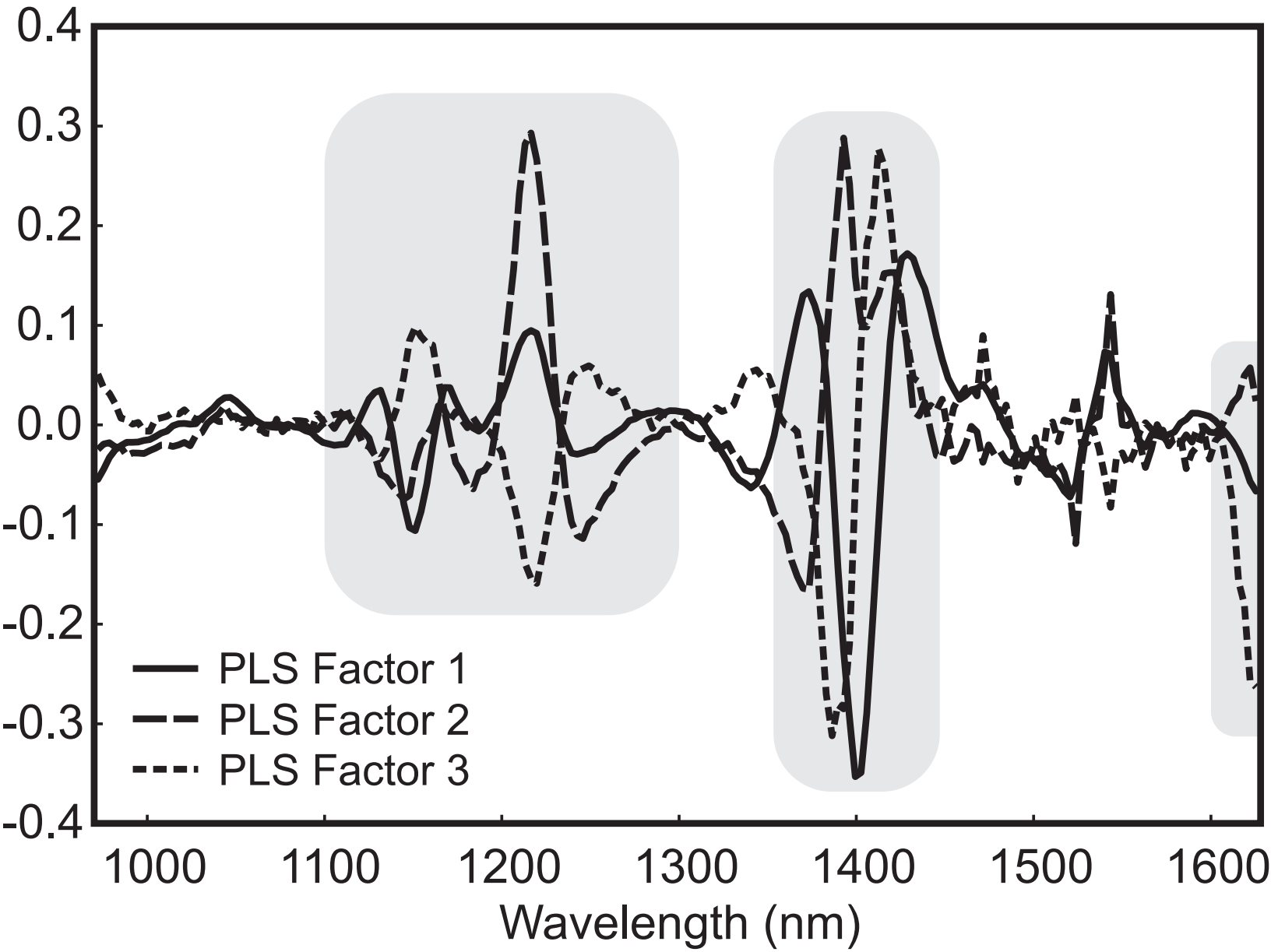
0.4
0.3
0.2
0.1
0.0
-0.1
-0.2
-0.3
-0.4
PLS Factor 1
PLS Factor 2
PLS Factor 3
1000
1100
1200
1300
1400
1500
1600
Wavelength (nm)